

Figure S1. Glycosylation of inhibitory immune receptor is required for interaction with its ligand, Related to Figure 1. (A) Western blot analysis of the indicated proteins shown in Figure 1 with commercially available antibodies. (B) Glycoprotein staining of purified His-tagged proteins with or without PNGase F treatment (top). Coomassie blue staining panel represents total amount of His-tagged proteins (bottom). Control (-), a control for non-glycoprotein; Control (+), a control for glycoprotein. CTRL, control. (C) Western blot analysis of PD-L1 in MDA-MB-231 and A431 cells with the absence or presence of N-linked or O-linked inhibitors. (D) N-linked glycosylation is required for PD-L1 and PD-1 interaction. Purified PD-L1 was treated with PNGaseF, Endonuclease H, or O-glyconase prior to the PD-1 binding assay. All error bars are expressed as mean \pm S.D. of 3 independent experiments.

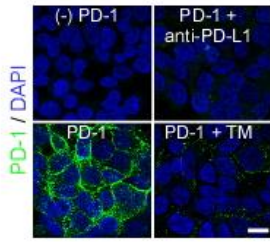
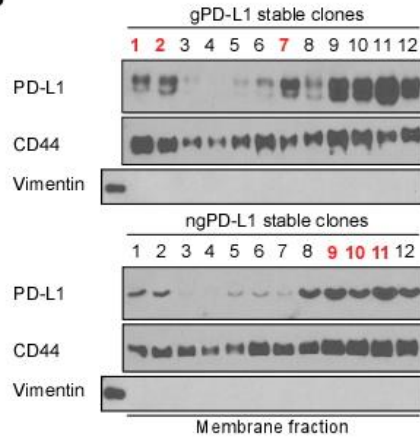
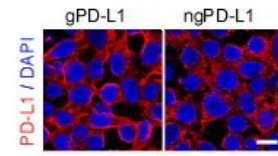
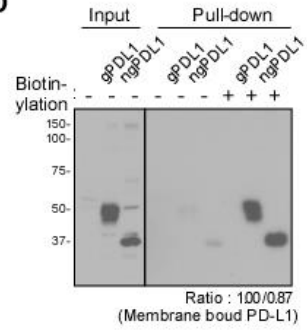
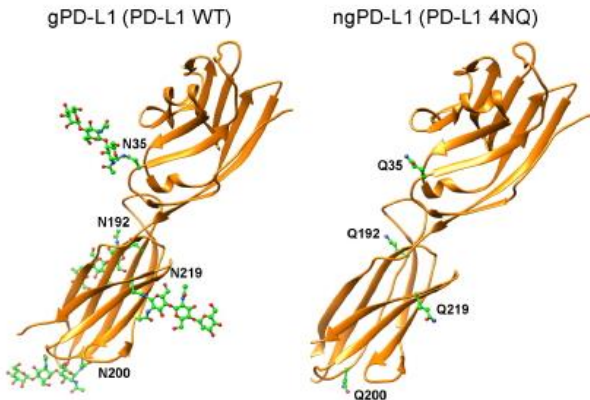
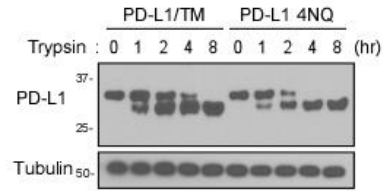
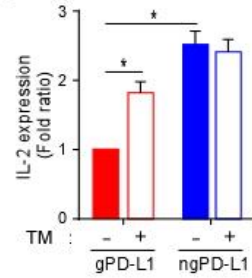
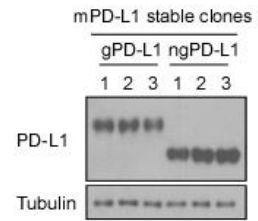
A**B****C****D****E****F****G****H**

Figure S2. Glycosylation of PD-L1 is required for interaction with PD-1, Related to Figure 2. (A) Interaction of PD-1 and PD-L1 proteins with or without TM or anti-PD-L1 antibody treatment. Confocal image shows bound PD-1/Fc fusion protein on membrane of gPD-L1 expressing BT549 cells. Cells were pretreated with MG132 prior to experiment. (B) Western blot analysis of PD-L1 in gPD-L1 or ngPD-L1 expressing BT549 clones. Red colored clones were used for PD-1 binding assay in Figure 2D. CD44 served as a marker of membrane fraction. Vimentin serves as a marker of cytoplasmic fraction. (C) Confocal image shows membrane localized gPD-L1 or ngPD-L1 proteins. (D) Membrane localization of gPD-L1 or ngPD-L1 proteins in BT549 cells. After biotinylation of membrane localization of gPD-L1 or ngPD-L1 proteins, the biotinylated proteins were pull-downed by streptavidin agarose. Membrane localized PD-L1 proteins were examined by Western blot. The ratio of membrane bound PD-L1 proteins was quantified by a densitometer (bottom). (E) Predicted structure of PD-L1 protein. Ribbon diagram of the PD-L1 and PD-1 complex. PD-L1 and PD-1 are shown in orange and blue, respectively. N-linked oligosaccharides are shown as sticks. Four glycosylation sites (N35, N192, N200 and N219) are shown as indicated. (F) Conformational changes of PD-L1 WT and 4NQ. Tunicamycin treated non-glycosylated PD-L1 WT (PD-L1/TM) and PD-L1 4NQ were treated with 10 nM trypsin and analyzed by Western blot. (G) Levels of soluble IL-2 in co-culture of Jurkat T cells and PD-L1 expressing BT549 cells. (H) Western blot analysis of PD-L1 in mouse gPD-L1 or ngPD-L1 expressing 4T1 clones. mPD-L1, mouse PD-L1. *p <0.05, statistically significant by Student's *t*-test. All error bars are expressed as mean \pm S.D. of 3 independent experiments.

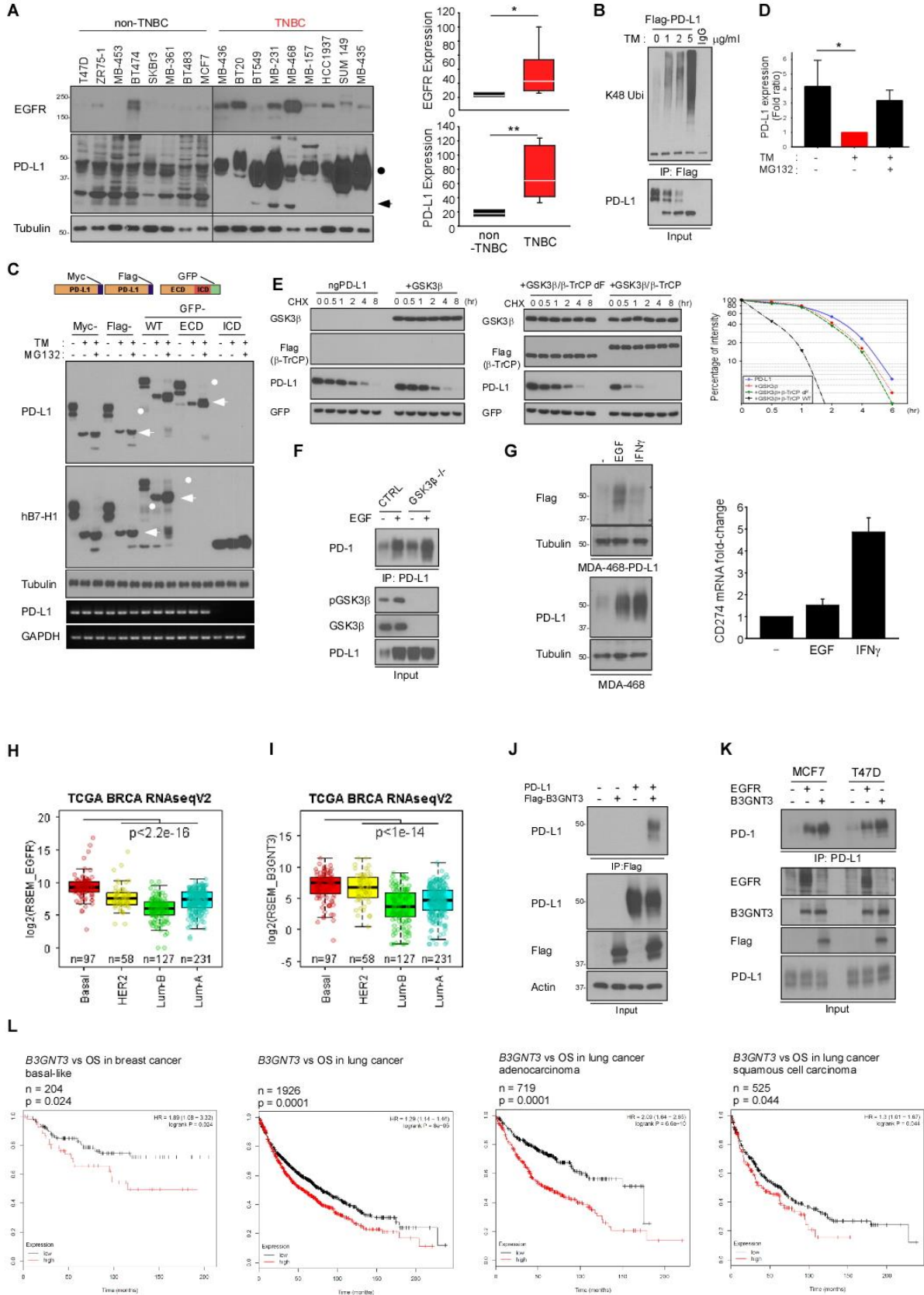


Figure S3. EGF signaling upregulates N-glycosyltransferase B3GNT3 in BLBC, Related to Figure 3. (A) Western blot analysis of EGFR and PD-L1 expression in a panel of non-triple negative and triple negative breast cancer cell lines. Quantification of EGFR and glycosylated PD-L1 are shown on the right. (B) Ubiquitination assay of PD-L1 in response to treatment with TM. HEK293 cells were transiently transfected with indicated constructs. Ubiquitinated PD-L1 was immunoprecipitated (IP) and subjected to Western blot analysis with the anti-ubiquitin K48 antibody. (C) Western blot analysis of PD-L1-Myc, PD-L1-Flag, PD-L1-GFP WT, extracellular domain (ECD), and intracellular domain (ICD) proteins in tunicamycin (TM) and/or MG132 treated cells. mRNA expressions are showed in bottom. (D) The intensity of glycosylated or non-glycosylated PD-L1 protein in (C) was quantified by a densitometer (bottom). (E) Protein stability of PD-L1 proteins in ngPD-L1 expressing BT549 cells. Cells were treated with 20 mM cycloheximide (CHX) at indicated intervals and analyzed in Western blot analysis. The intensity of PD-L1 protein was quantified by a densitometer (bottom). (F) PD-L1 and PD-1 binding analysis in vitro. Wild-type and GSK3 β deficient mouse embryonic fibroblast (MEF) cells were transient transfected with Flag-tagged PD-L1. PD-L1 was immunoprecipitated and subject to in vitro binding with PD-1. (G) Western blot analysis of PD-L1 expression in MDA-MB-468 and MDA-MB-468-PD-L1 cells upon EGF or IFN γ treatment. Cells were serum starved overnight prior to EGF or IFN γ treatment for 6 h. qPCR analysis of PD-L1 is shown on the right. (H) Boxplot of EGFR expression in breast cancer subtypes using TCGA RNAseq_V2 data, Student's t test was used to evaluate significant increases of EGFR expression in basal vs other subtypes (I) Box plot of B3GNT3 expression in breast cancer subtypes. (J) Co-immunoprecipitation of PD-L1 and B3GNT3. HEK 293 cells were transient transfected with Flag-B3GNT3 and/or PD-L1. Cell lysates were IP with Flag antibody and subsequently western blot with PD-L1. (K) PD-L1 and PD-1 binding in non-TNBC cell lines. MCF7 or T47D non-TNBC cells were transiently transfected with Flag-B3GNT3 and/or EGFR. Cell lysates were then subjected to IP with PD-L1 antibody followed by Western blotting with PD-1 antibody. (L) Kaplan-Meier overall survival curves of *B3GNT3* expression in breast or lung cancer TCGA dataset. *p <0.05, **p <0.001, statistically significant by Student's *t*-test. All error bars are expressed as mean \pm S.D. of 3 independent experiments.

Table S1. Gene expression profile of N-linked glycotransferase, Related to Figure 3.

GeneCard ID	Gene name	Symbol	Expression in TNBC (medianFC)	Correlation with EGFR (PearsonR)
GC22P039447	Mannosyl (Beta-1,4-)-Glycoprotein Beta-1,4-N-Acetylglucosaminyltransferase	MGAT3	3.08	0.5246
GC19P017794	UDP-GlcNAc:BetaGal Beta-1,3-N-Acetylglucosaminyltransferase 3	B3GNT3	6.22	0.4426
GC12M101745	N-Acetylglucosamine-1-Phosphate Transferase Alpha And Beta Subunits	GNPTAB	1.21	0.436
GC03P186930	ST6 Beta-Galactoside Alpha-2,6-Sialyltransferase 1	ST6GAL1	1.73	0.3848
GC19M012649	Mannosidase Alpha Class 2B Member 1	MAN2B1	1.4	0.3673
GC15P092393	ST8 Alpha-N-Acetyl-Neuraminide Alpha-2,8-Sialyltransferase 2	ST8SIA2	0.87	0.2992
GC02P128091	UDP-Glucose Glycoprotein Glucosyltransferase 1	UGGT1	1.09	0.2794
GC05M100806	ST8 Alpha-N-Acetyl-Neuraminide Alpha-2,8-Sialyltransferase 4	ST8SIA4	1.04	0.2976
GC01P043978	Beta-1,4-Galactosyltransferase 2	B4GALT2	1.68	0.2185
GC02P134119	Mannosyl (Alpha-1,6-)-Glycoprotein Beta-1,6-N-Acetyl-Glucosaminyltransferase	MGAT5	0.97	0.3076
GC02M074461	Mannosyl-Oligosaccharide Glucosidase	MOGS	1.53	0.2073
GC05M180790	Mannosyl (Alpha-1,3-)-Glycoprotein Beta-1,2-N-Acetylglucosaminyltransferase	MGAT1	1.06	0.272
GC17P076868	Mannosyl (Alpha-1,6-)-Glycoprotein Beta-1,6-N-Acetyl-Glucosaminyltransferase	MGAT5B	1.25	0.2036
GC09M033100	Beta-1,4-Galactosyltransferase 1	B4GALT1	1.05	0.1495
GC02P062196	UDP-GlcNAc:BetaGal Beta-1,3-N-Acetylglucosaminyltransferase 2	B3GNT2	1.04	0.1342
GC01P117367	Mannosidase Alpha Class 1A Member 2	MAN1A2	0.88	0.207
GC10P073772	Fucosyltransferase 11	FUT11	0.8	0.1359
GC01M161171	Beta-1,4-Galactosyltransferase 3	B4GALT3	1.27	0.0767
GC03M033013	Galactosidase Beta 1	GLB1	1.05	0.1662
GC05M179797	Mannosyl (Alpha-1,3-)-Glycoprotein Beta-1,4-N-Acetylglucosaminyltransferase	MGAT4B	1.21	0.1268
GC11M062756	Glucosidase II Alpha Subunit	GANAB	1.09	0.1623
GC19P011435	Protein Kinase C Substrate 80K-H	PRKCSH	1.19	0.0404
GC12M085955	MGAT4 Family Member C	MGAT4C	1	0.1006
GC11P074988	Neuraminidase 3	NEU3	0.91	0.1
GC02P241808	Neuraminidase 4	NEU4	0.6	0.0417
GC06M119269	Mannosidase Alpha Class 1A Member 1	MAN1A1	0.52	0.0804
GC18P057350	ST8 Alpha-N-Acetyl-Neuraminide Alpha-2,8-Sialyltransferase 3	ST8SIA3	1	0.031
GC02P233032	Neuraminidase 2	NEU2	1	0.0786
GC14P049620	Mannosyl (Alpha-1,6-)-Glycoprotein Beta-1,2-N-Acetylglucosaminyltransferase	MGAT2	0.89	-0.0099
GC13M095801	UDP-Glucose Glycoprotein Glucosyltransferase 2	UGGT2	0.92	0.0018
GC20M035115	ER Degradation Enhancing Alpha-Mannosidase Like Protein 2	EDEM2	1.19	-0.0351
GC15M072340	Hexosaminidase Subunit Alpha	HEXA	0.99	0.0416
GC06M143494	Fucosidase, Alpha-L- 2	FUCA2	1.09	-0.021
GC09P137086	Mannosidase Alpha Class 1B Member 1	MAN1B1	0.96	-0.0188
GC15P090902	Mannosidase Alpha Class 2A Member 2	MAN2A2	1.06	0.072
GC10M017360	ST8 Alpha-N-Acetyl-Neuraminide Alpha-2,8-Sialyltransferase 6	ST8SIA6	0.08	-0.0697
GC03P005203	ER Degradation Enhancing Alpha-Mannosidase Like Protein 1	EDEM1	0.71	-0.0901
GC05P074640	Hexosaminidase Subunit Beta	HEXB	0.85	-0.0348
GC04M102631	Mannosidase Beta	MANBA	0.85	-0.1086
GC16M005014	N-Acetylglucosamine-1-Phosphodiester Alpha-N-Acetylglucosaminidase	NAGPA	1.04	-0.1493
GC04M177430	Asparlyglucosaminidase	AGA	0.75	-0.2059
GC02M098700	Mannosyl (Alpha-1,3-)-Glycoprotein Beta-1,4-N-Acetylglucosaminyltransferase, Isozyme A	MGAT4A	0.59	-0.21
GC19M041425	UDP-GlcNAc:BetaGal Beta-1,3-N-Acetylglucosaminyltransferase 8	B3GNT8	0.41	-0.1747
GC01M184659	ER Degradation Enhancing Alpha-Mannosidase Like Protein 3	EDEM3	0.69	-0.1536
GC06M031857	Neuraminidase 1	NEU1	0.93	-0.248
GC01P025628	Mannosidase Alpha Class 1C Member 1	MAN1C1	0.36	-0.1886
GC01M023845	Fucosidase, Alpha-L- 1	FUCA1	0.52	-0.2878
GC16P001351	N-Acetylglucosamine-1-Phosphate Transferase Gamma Subunit	GNPTG	0.69	-0.3938
GC14P065411	Fucosyltransferase 8	FUT8	0.31	-0.3535

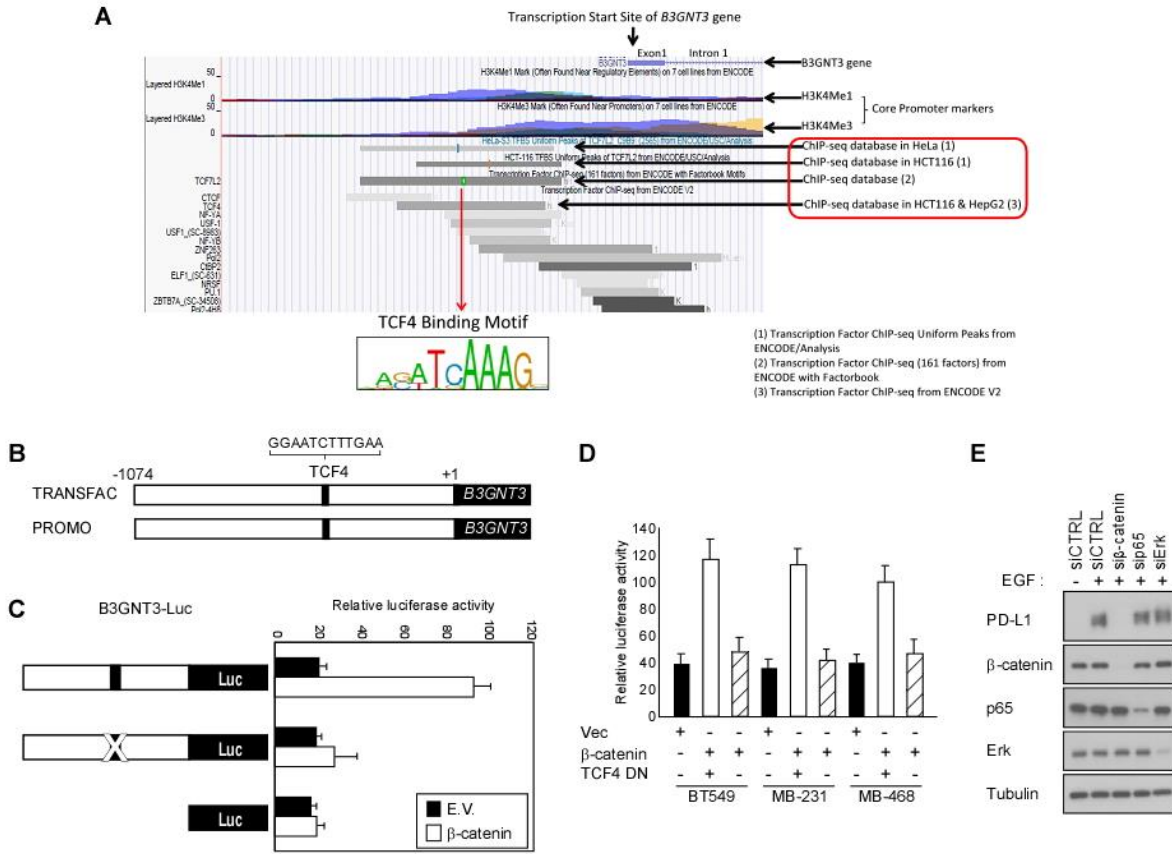


Figure S4. EGF signaling upregulates glycosyltransferase *B3GNT3* via β -catenin pathway, Related to Figure 4. (A) ENCODE database analysis of TCF4 transcription factor on the *B3GNT3* promoter region using chromatin immunoprecipitation sequencing. (B) TCF4 binding motif analysis of the *B3GNT3* promoter using the TRANSFAC and PROMO databases. (C) *B3GNT3* promoter luciferase assay was performed by transient transfection in HEK293 cells. (D) *B3GNT3* promoter assay in presence of 10 ng/ml EGF, β -catenin and/or TCF4 DN (dominant negative TCF4). (E) Western blot analysis of glycosylated PD-L1 proteins in β -catenin, p65, or Erk knocking down cells with EGF treatment. Error bars represent mean \pm S.D. of 3 independent experiments.

Table S2. Analysis of lectin binding affinity to PD-L1 protein, Related to Figure 4.

Lectin (FITC conjugated)	Abbreviation	PD-L1 binding			PD-L1 WT specific binding
		WT/M2	4NQ/M2	M2	
Concanavain A	Con A	+	+	+	-
Peanut	PNA	-	-	-	-
<i>Dolichos biflorus</i>	DBA	-	-	-	-
<i>Ricinus communis</i> I	RCA 120	+	+	+	-
Soybean	SBA	-	-	-	-
Wheat Germ	WGA	+	+	+	-
<i>Ulex europaeus</i> I	UEA I	-	-	-	-
<i>Griffonia simplicifolia</i> I	GSL I	+	-	-	+
<i>Phaseolus vulgaris</i> Erythroagglutinin	PHA-E	+	+	+	-
<i>Lens culinaris</i>	LCA	+	+	+	-
Succinylated Wheat Germ	S-WGA	+	-	-	+
<i>Pisum sativum</i>	PSA	+	+	+	-
<i>Griffonia simplicifolia</i> II	GSL II	+	-	-	+
<i>Erythrina cristagalli</i>	ECL	-	-	-	-
<i>Datura stramonium</i>	DSL	+	+	+	-
Jacalin	Jacalin	+	+	+	-
<i>Lycopersicon esculentum</i>	LEL	+	-	-	+
<i>Vicia villosa</i>	VVA	+	-	-	+
<i>Solanum tuberosum</i>	STL	+	+	+	-

WT/M2, PD-L1 WT protein on M2 (anti-Flag) agarose; 4NQ/M2, PD-L1 4NQ protein on M2 (anti-Flag) agarose; M2, M2 (anti-Flag) agarose.

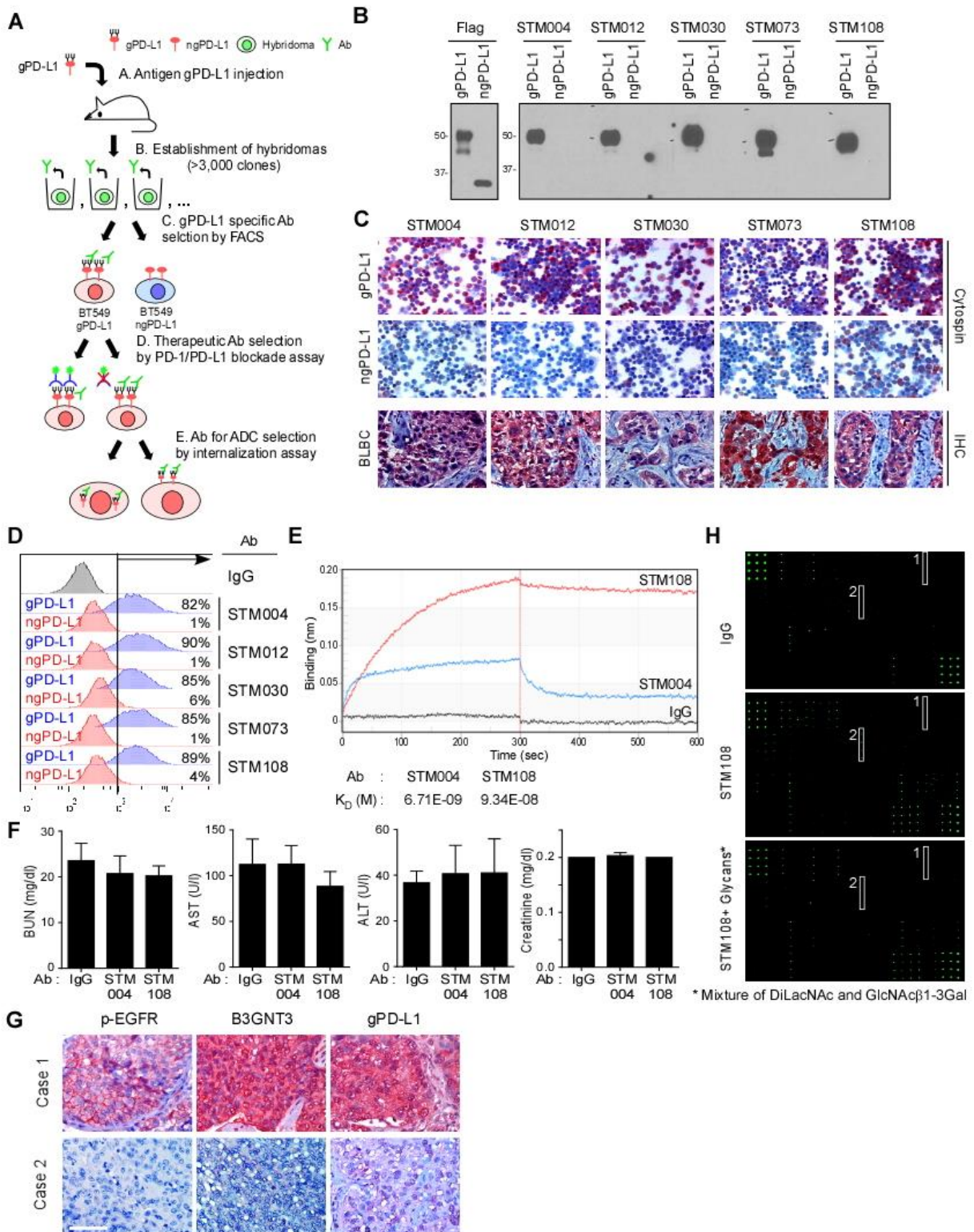


Figure S5. Production and validation of glycosylated PD-L1 antibody, Related to Figure 5.

(A) Working flow chart for production of glycosylated PD-L1 antibody. (B) Western blot analysis of PD-L1 by anti-Flag or glycosylated PD-L1 antibodies in gPD-L1 or ngPD-L1 expressing BT549 cell lysates. (C) Validation of glycosylated PD-L1 antibodies for cytospin staining or immunohistochemical staining of basal-like breast cancer (BLBC) tissues. (D) Flow cytometer analysis by glycosylated PD-L1 antibodies in gPD-L1 or ngPD-L1 expressing BT549 cells. IgG serves as a negative control. (E) Binding affinity (K_D) analysis of glycosylated PD-L1 antibodies, STM004 and STM108 by Octet. (F) The effect of treatment on BALB/c mice. Mice liver, and kidney functions were measured at the end of the experiments. AST, aspartate aminotransferase; ALT, alanine aminotransferase; BUN, blood urea nitrogen. (G) IHC staining of human breast cancer patient samples of p-EGFR, B3GNT3 and gPD-L1. (H) Representative images for the Glycan Array. The Glycan Array 100 was probed with biotin-labeled STM108 antibody. STM108 binds to two glycans (1 and 2) and the bindings are compromised by mixture of B3GNT3 substrate or product, mixture of DiLacNAc and GlcNAc β 1-3Gal. All error bars are expressed as mean \pm S.D. of 3 independent experiments.

Table S3. Characterization of gPD-L1 antibodies, Related to Figure 5.

	STM004	STM108
Recognizing glycosylation site	N35	N192, N200
PD-1/PD-L1 blockade activity (EC50, μ g/ml)	0.138	0.036
K_D (affinity, M)	9.34E-08	6.71E-09
Internalization	-	+++
Enhancement of T cell killing activity	++	+++
Epitope binding site of PD-L1	Y56, K62, K75	S80, Y81, K162, S169

Table S4. Relationship between gPD-L1, pEGFR (Y1068), and B3GNT3 expression in surgical specimens of breast cancer, Related to Figure 5.

		Expression of gPD-L1			p value
		- / +	++ /+++	Total	
pEGFR		31	33	64	p = 0.027*
	- / +	(72.1%) 12	(50.8%) 32	(59.3%) 44	
	++ /+++	(27.9%) 43	(49.2%) 65	(40.7%) 108	
	Total	(100%)	(100%)	(100%)	
B3GNT3		25	32	57	p = 0.002*
	- / +	(75.8%) 8	(43.2%) 42	(53.3%) 50	
	++ /+++	(24.2%) 33	(56.8%) 74	(46.7%) 107	
	Total	(100%)	(100%)	(100%)	

*Correlations were analyzed using the PASS Pearson Chi-Square test. A p value < 0.05 was set as the criterion for statistical significance. A p value of < 0.05 was set as the criterion for statistical significance.

Movie S1. An example STM108 trajectory measured on the membrane of a BT549 cell, Related to Figure 6. A single labeled anti-gPD-L1 antibody was tracked for 400 sec. The movie playback rate is 50×. The cell size is approximately $35\ \mu\text{m} \times 35\ \mu\text{m} \times 10\ \mu\text{m}$ (xyz). The cell membrane is plotted as a red iso-surface while the nucleus is a blue iso-surface. Trajectory is rainbow colored with magenta denoting the beginning.

Movie S2. An example STM004 trajectory measured on the membrane of a BT549 cell, Related to Figure 6. A single labeled anti-gPD-L1 antibody was tracked for 400 sec. The movie playback rate is 50×. The cell size is approximately $22\ \mu\text{m} \times 22\ \mu\text{m} \times 10\ \mu\text{m}$ (xyz). The cell membrane is plotted as a red iso-surface while the nucleus is a blue iso-surface. Trajectory is rainbow colored with magenta denoting the beginning.

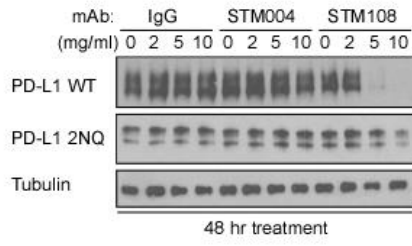
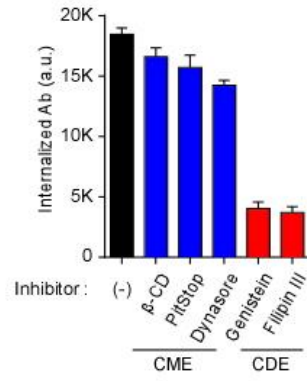
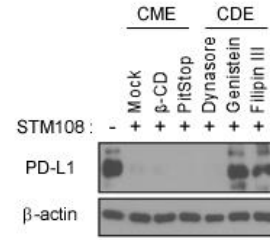
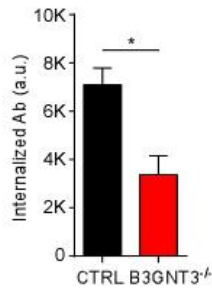
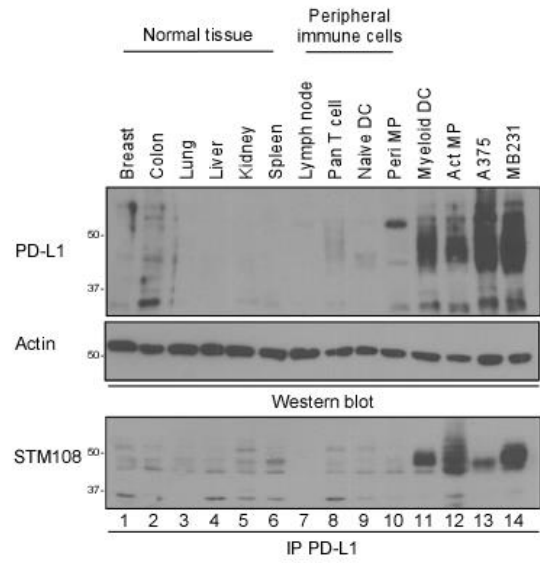
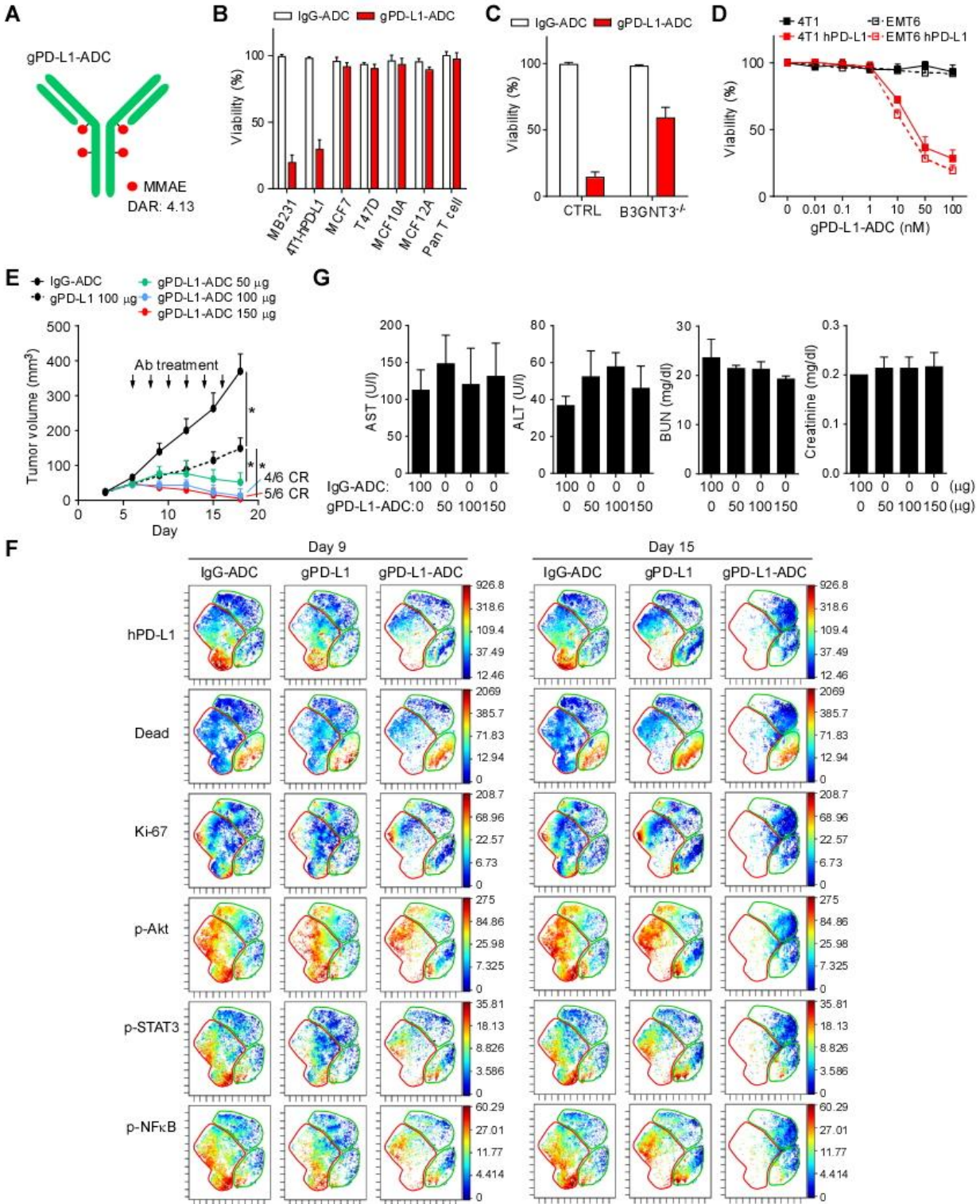
A**B****C****D****E**

Figure S6. gPD-L1 antibody STM108 induces internalization and degradation of PD-L1, Related to Figure 6. (A) Western blot analysis of wild-type (WT) PD-L1 or 2NQ mutant PD-L1 after treatment with IgG, STM004, or STM108. (B) Internalization of STM108 in clathrin-mediated endocytosis (CME) or caveolae-dependent endocytosis (CDE) inhibitors treated cells. STM108 was labeled with pHrodoTM Red and then add to PD-L1 WT expressing MB231 cells. Internalized antibodies are quantified at 12 hours. (C) Western blot analysis of wild-type (WT) PD-L1 in STM108 and/or CME or CDE inhibitors treated PD-L1 WT expressing MB231 cells. (D) Internalization of STM108 in STM108 treated PD-L1 WT expressing control (CTRL) or B3GNT3 knockout (B3GNT3^{-/-}) BT549 cells. (E) Western blot analysis of PD-L1 and STM108 in normal tissues, peripheral immune cells, and cancer cell lysates. Protein lysates (1 μ g) were separated on SDS-PAGE for Western blot analysis. Myeloid DC, myeloid dendritic cells. Act MP, tumor-associated macrophage. Arrowhead, non-glycosylated PD-L1. Closed circle, glycosylated PD-L1. Lower panel, PD-L1 was immunoprecipitated and then subjected to Western blotting using STM108. *p <0.05, statistically significant by Student's *t*-test. All error bars are expressed as mean \pm S.D. of 3 independent experiments.



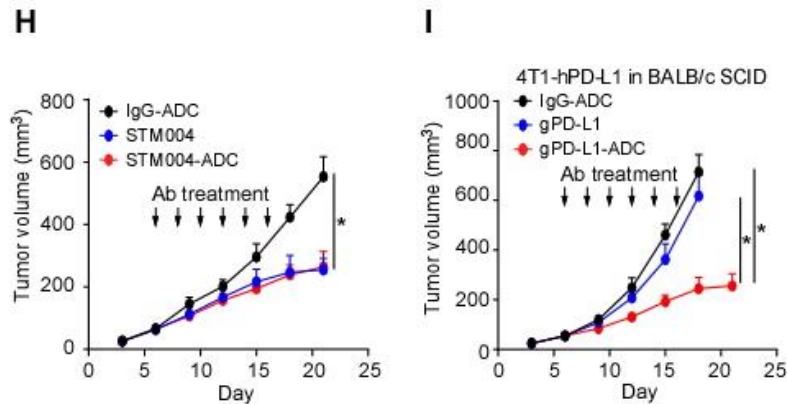


Figure S7. gPD-L1 antibody-drug conjugate (gPD-L1-ADC) shows PD-L1/PD-1 blockade and cytotoxicity in 4T1-hPD-L1 syngeneic mouse model, Related to Figure 7. (A) Schematic diagram of STM108 antibody-MMAE conjugate (gPD-L1-ADC). DAR, drug-to-antibody ratio. (B, C) Cell viability was measured after 50 nM gPD-L1-ADC treatment at 72 h. (D) Cytotoxic profile of gPD-L1-ADC in human PD-L1 (hPD-L1) expressing 4T1 or EMT6 cells. Cell viability were measured at 72 h. (E) The tumor growth of human PD-L1 expressing 4T1 (4T1-hPD-L1) cells in IgG-ADC, gPD-L1 (STM108), or gPD-L1-ADC antibody treated BALB/c mice. Tumors were measured at the indicated time points and dissected at endpoint. $n = 7$ mice per group. Antibodies was injected intraperitoneally on days 6, 8, 10, 12, 14, and 16 after 4T1-hPD-L1 cells inoculation. CR, complete regression. (F) viSNE map derived from CyTOF (7-marker) analysis of 4T1-hPD-L1 tumors at day 9 and 15. Tumor cell populations were identified as hPD-L1 marker. Cells in the map are colored by the intensity of expression of the indicated markers. (G) The effect of treatment on BALB/c mice. Mice liver, and kidney functions were measured at the end of the experiments. AST, aspartate aminotransferase; ALT, alanine aminotransferase; BUN, blood urea nitrogen. (H) The tumor growth of 4T1-hPD-L1 cells in IgG-ADC, STM004, or STM004-ADC antibody treated BALB/c mice. Tumors were measured at the indicated time points and dissected at endpoint. $n = 7$ mice per group. Arrow, antibody (Ab) treatment. (I) The tumor growth of 4T1-hPD-L1 cells in IgG-ADC, gPD-L1 (STM108), or gPD-L1-ADC antibody treated BALB/c SCID mice. Tumors were measured at the indicated time points and dissected at endpoint. $n = 7$ mice per group. Arrow, antibody (Ab) treatment. * $p < 0.05$, statistically significant by Student's t -test. All error bars are expressed as mean \pm S.D. of 3 independent experiments.

Table S5. Antibodies used for Cy-TOF analysis, Related to Figure 7.

Marker	Clone	Label
hPD-L1	E1L3N	164Dy
gPD-L1	STM108	155Gd
p-NF κ B	93H1	149Sm
p-STAT3	M9C6	152Sm
p-AKT	M89-61	159Tb
Ki67	Ki67	168Er
EpCam	G8.8	166Er
Cisplatin		195Pt